Macromolecular Materials and Engineering
www.mame-journal.de

A Superabsorbent Sodium Polyacrylate Printing Resin as Actuator Material in 4D Printing

*Lukas Hiendlmeier, Tetsuhiko F. Teshima, Francisco Zurita, Heike Url, Philipp Rinklin, and Bernhard Wolfrum**

Superabsorbent polymers are materials that exhibit a high swelling behavior in liquids and can hold the absorbed liquid even against externally applied pressure. They are commercially used, for example, in baby diapers, fake snow, or swellable children's toys. Most commercially available superabsorbent polymers are based on polymerized and crosslinked sodium acrylate. Here, a material formulation to create 3D objects using stereolithographic printing of sodium acrylate is demonstrated. The material shows typical superabsorbent properties that cannot be reached with conventional 3D printing materials. The printed structures swell strongly (up to 20 times in weight) in aqueous environments and still show 65% of the swelling under an external load of 100 kPa. This swelling can be used for 3D printed parts that can automatically change their size or shape when exposed to water. To show the versatility of this approach, selected structures are 3D printed, including a ship and a medical stent. Also the applicability of actuation by printing a structure is demonstrated, which deforms to a self-closing container upon exposure to water.

1. Introduction

Additive manufacturing has seen a rapid increase in applications over the last decades. This development has been primarily motivated by several advantages of 3D printing techniques, such as the ability to fabricate customized complex structures with freedom of design at low material consumption compared to traditional manufacturing. A commonly used method of additive manufacturing is stereolithographic printing (SLA). In this technique, a liquid photosensitive resin is polymerized layer by layer to the designed shape by a structured light source, such as a laser scanner or a dynamic mirror array.[1–3] An extension of classical additive manufacturing is 4D printing, a term proposed in 2013 by Tibbits for using smart materials in structures that can change shape or other properties over time because of an interaction with external stimuli.[2,4–7] For example, a change in size can lead to the deformation of a 3D printed device because of the resulting internal stress. By combining multiple materials in one printed structure, complex deformations can be generated without the need for different mechanical parts, like joints or gears. Examples of such multi-material structures are printed bilayers composed of a water swelling and a non-swelling but flexible material that fold when immersed in water. This technique has been used to develop, for example, grippers or a self-folding box.[8–14] The possibility of miniaturizing such moving structures and the broad selection of soft materials is particularly beneficial in biomedical engineering or soft robotics.[15–19]

Stimuli-responsive materials for 4D printing often use the shape memory effect or swelling in a medium as a driving force, like hydrogels in water.[2,7,14,20] While the swelling behavior of some hydrogels is solely triggered in the presence of water,[21–23] other materials can react to different external factors such as temperature and light (e.g., poly(N-isopropylacrylamide) called PNIPAm),[11–13,24,25] an electric field,[26–29] or a change in pH (polyacrylic acid).[30–32] It is often beneficial if the hydrogel material exhibits a strong swelling behavior—a high swelling ratio as well as the ability to expand against external pressure—to use hydrogels as actuators in 4D printed parts.[33,34] The strong swelling against an external pressure is crucial for strongly deforming structures, or structures that can hold a load, such as grippers. Several examples of highly swelling 3D printing resins have already been reported in the literature, such as mixtures of Pluronic F127 and acrylic acid showing swelling up to 71 times their initial weight.[35] Another hydrogel based on acrylic

L. Hiendlmeier, T. F. Teshima, F. Zurita, H. Url, P. Rinklin, B. Wolfrum
Neuroelectronics, Munich Institute of Biomedical Engineering, Department of Electrical Engineering, TUM School of Computation, Information and Technology
Technische Universität München
Boltzmannstraße 11, 85748 Garching, Germany
E-mail: bernhard.wolfrum@tum.de
L. Hiendlmeier, T. F. Teshima, F. Zurita, B. Wolfrum
Medical & Health Informatics Laboratories
NTT Research Incorporated
940 Stewart Dr, Sunnyvale, CA 94085, USA

The ORCID identification number(s) for the author(s) of this article can be found under https://doi.org/10.1002/mame.202200306

DOI: 10.1002/mame.202200306

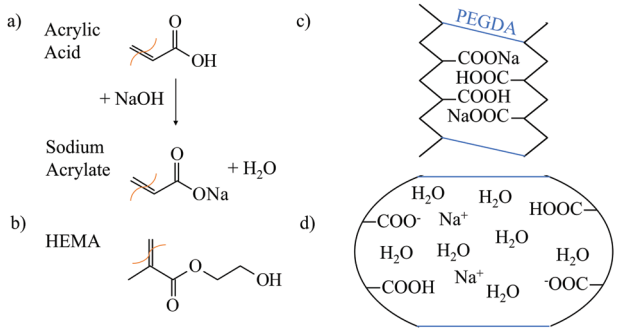

Figure 1. Molecular representation of superabsorbent polymer. a) Chemical structure and neutralization reaction with NaOH. b) Chemical structure of HEMA as a second monomer. c) Schematic representation of the polymerized hydrogel network in a non-swollen state. d) Swollen polymer network with dissolved ions resulting in an uptake of water due to osmosis.

acid shows pH-sensitive swelling to 20-fold its weight after being dried from the printed state.[32] So far, the investigation of swelling behavior in the presence of an external load has not been the focus of most 4D printing publications. Exceptions are a reported PNIPAm hydrogel, which could produce 80 kPa of maximal swelling pressure,[36] and a reinforced thermosensitive PNIPAm hydrogel, which generated 10 kPa while shrinking.[9]

Crosslinked sodium polyacrylate is a hydrogel material showing strong swelling properties also against an external load. This material is commonly called "superabsorbent" as it exhibits swelling up to 285 times its initial weight in the presence of water.[37–40] It finds commercial applications in baby diapers, children's toys, or fake snow. Sodium polyacrylate superabsorbent polymers are generated by partly neutralizing acrylic acid (**Figure 1**a) with sodium hydroxide. The sodium ion (Na^+) binds to the acid's OH group, forming the sodium acrylate salt (Figure 1b). Due to the acrylate group's C–C double-bond, the molecules can undergo radical polymerization forming sodium polyacrylate. A crosslinked polymer network is formed with a diacrylate monomer, which is not dissolvable in water in contrast to not crosslinked sodium polyacrylate. Na^+ ions are released upon exposure to water but stay within the network because of the remaining negative charge. The resulting dissolved ions generate an osmotic pressure, which draws water into the polymer network and causes the strong swelling behavior of the hydrogel. The high osmotic pressure, compared to other hydrogels, renders sodium polyacrylate a suitable base material to actuate 4D printed structures, allowing deformations against an external load.[41]

In this work, we developed an SLA printable resin based on acrylic acid and sodium acrylate to use superabsorbent properties in printed structures. We demonstrated the 3D printing of complex structures and investigated the swelling behavior of our materials in different solutions. Furthermore, we characterized the mechanical properties, investigated the force generation during swelling, and tested the material's biocompatibility for potential biomedical applications. Finally, we demonstrated the printing of a self-folding cage by printing joined layers of two different materials.

2. Results

2.1. Resin Development

The usual synthesis of sodium polyacrylate superabsorbent polymers involves radical polymerization of acrylates, which is also the primary polymerization method in SLA 3D printing.[1,42] Therefore, we used identical base monomers to develop an ultraviolet light (UV) sensitive 3D printable resin. Hydrogel resins printed with acrylic acid are usually mixed with water as a diluent to final concentrations of 10–30%.[30,32] Here, the aim was to develop a resin with lower water content for two reasons: first, a low water content in the printed material results in a high degree of swelling capability directly after printing without the need to dry the printed structure. This is advantageous because drying can lead to unwanted deformations depending on the geometrical structure in multi-material samples. Second, water-soluble photoinitiators, which are usually expensive and have low activity, would add additional constraints on the resin development.[43] Ultimately, we used 1% Omnirad 2100, which showed sufficient reactivity for printing and was easily dissolvable in the resin given a sufficiently low water content. Furthermore, we dissolved 2-isopropylthioxanthone (ITX) as a photoabsorber and 2,2,6,6-tetramethylpiperidine-1-oxyl (TEMPO) as a polymerization quencher in the resin to enhance the printing resolution. ITX is a type II photoinitiator with an absorption maximum at 380 nm. It limits the penetration depth of the print exposure preventing over curing of the print in the deeper layers. It thereby increases the print resolution perpendicular to the print layer without initiating additional polymerization of the resin, since there is no amine group present in the mixture. TEMPO molecules can terminate the radical polymerization and confine the polymerization just in the exposed areas, achieving better resolution within the build layer (Figure S1, Supporting Information). The sodium acrylate is generated by neutralizing the acrylic acid with sodium hydroxide (NaOH) to a mole degree of 37%.[39] As shown in Figure 1, water is generated in this reaction adding up to 26% w/w in the final mixture. This water content was necessary to dissolve sodium acrylate and prevent crystallization.

Acrylic acid is a reactive and fast polymerizing molecule, which by itself renders 3D printing challenging to control. Thus, mixing acrylic acid with a slower polymerizing monomer containing methacrylic groups can give a well-controlled printing performance.[44] Further, this mixture results in a better interlayer adhesion as more unreacted methacrylic functional groups than acrylate groups remain after curing a layer. These unreacted groups can link to subsequently printed layers. We chose 2-hydroxyethyl methacrylate (HEMA) as a methacrylate monomer. It mixes well with acrylic acid and water, forms a biocompatible hydrogel, and does not interfere with the swelling of the sodium polyacrylate.[45] Resin mixtures without adding HEMA showed spontaneous polymerization during the preparation and were therefore not usable (Table S1, Supporting Information).

The composition of the primary monomers after the neutralization reaction is summarized in **Table 1**, with the resins named SAP 37/X. The base monomers all have a single acrylic group, polymerize as a linear polymer chain, and must be crosslinked to make the hydrogel insoluble in water. We used poly(ethylene glycol) diacrylate (PEGDA, M_n 525) with two acrylate groups as

Table 1. Composition of the 3D printing resins, after neutralizing the acrylic acid with the sodium hydroxide. The printing additives were added with respect to the weight of the base monomer mixture.

w/w		SAP 37/X
Base monomers	Acrylic acid	29%
	Sodium acrylate	22%
	Water	26%
	HEMA	23%
Additives	PEGDA 525	0.5%, 1%, 5%
	Omnirad 2100	1%
	ITX	0.05%
	TEMPO	0.02%

a crosslinker since it is more hydrophilic than shorter PEGDA chains forming a biocompatible hydrogel.[46]

2.2. 3D Printing of Superabsorbent Material

The SAP 37/1 resin achieved reliable printing of down to 0.4 mm sized features (Figure S2, Supporting Information). We printed a ship and a stent-like mesh structure, as shown in **Figure 2**. Further printed examples of different geometries are shown in Figure S3, Supporting Information. The printed structures exhibited a high swelling when immersed in water, as expected from superabsorbent material. The images compare the devices directly after printing (small yellow part) to the same design after immersion in water (bigger structures in the back). A time-lapse video showing the swelling of the stent-like mesh structure can be found in Video S1, Supporting Information. During water immersion, thinner model parts swell much faster than thicker parts because the diffusion of the water into the material is the time-limiting factor. In designs with different wall thicknesses, this can lead to strong deformations and even rupture the material. The printed boat's interior was hollow and had a maximum wall diameter of 1 mm to avoid this effect, so all parts of the boat had a similar swelling speed. For structures with varying wall thicknesses, a stepwise swelling in decreasing salt solution can be done to prevent a rupture (Figure S3b, Supporting Information). The printed boat and the stent structures show a possible field of application for smart materials like the superabsorbent resin. Both parts must be transferred through a narrow opening (neck of the bottle or vascular system, respectively), and later expand to their desired shape or size.[47]

2.3. Swelling Characteristics

We measured the mass gain of printed 5 mm cubes after immersion into aqueous salt solutions (e.g., sodium chloride, NaCl) to quantify the swelling. Since the absorption mainly results from the osmotic pressure of the Na^+ ions inside the superabsorbent polymer networks, the swelling is expected to decrease with a higher salt concentration in the solution.[40,48] We also investigated the change in mass for differently crosslinked materials since a higher crosslinking degree is expected to cause a lower swelling.[48,49] Therefore, we mixed resins with concentrations of 0.5%, 1%, and 5% of PEGDA 525 (SAP 37/05, SAP 37/1, and SAP 37/5, respectively). **Figure 3** shows the relative change of mass ($\Delta m\ m_0^{-1}$) after immersion for 24 h compared to the mass of cubes directly after printing (m_0).

We investigated the mass change of the superabsorbent polymer after drying the printed cubes for 24 h in an evacuated desiccator with silica beads to emulate storing conditions in a lab environment. We observed a negligible change in mass after storage, which is surprising considering the water content of the printed resin (26%). At elevated temperatures (100 °C), the samples lost a higher amount of mass (SAP 37/1 18%). However, the slight decrease in the water content in the dry vacuum already rendered the parts rigid and brittle. After a minor swelling with a maximum increase of $\Delta m\ m_0^{-1} = 0.1 \pm 0.1$ in saturated NaCl solution for 24 h, the parts were flexible again. This change in stiffness can be caused by hydrogen bonding between the acrylic acid and the HEMA OH side groups. The hydrogen bonds dissociate with higher water content in the material, lowering the glass transition temperature and making it flexible.[50] This swelling in saturated solution was used to precondition stored, dried parts, before complete swelling in the final solution. The highest swelling occurred in pure water with $\Delta m\ m_0^{-1} = 21 \pm 3$ for the low crosslinked SAP 37/05 resin. The higher crosslinked resins SAP 37/1 and SAP 37/5 showed a mass increase of $\Delta m\ m_0^{-1} = 15 \pm 1$ and 5.8 ± 0.5,

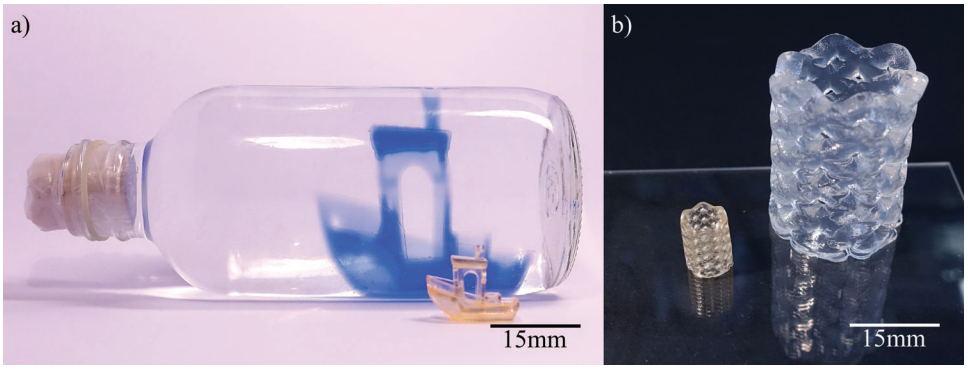

Figure 2. 3D printed superabsorbent structures in "as printed" and swollen states. a) A benchmarking model known as "Benchy" in the 3D printing community, was printed with SAP 37/1 at a length of 15 mm. In the front, it is shown as printed in the non-swollen state. The blue ship inside the flask was transferred through the narrow neck in this small state and then swollen in ink-dyed water to the full size. b) A stent-like mesh structure from SAP 37/05 as printed and after swelling for 1 h in water.

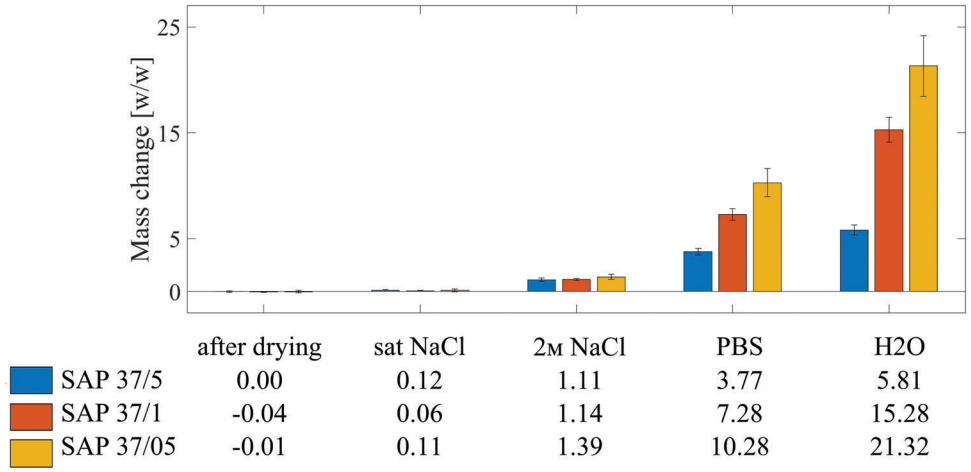

Figure 3. Mass change (mean and standard deviation, $n = 15$) of 5 mm cubes from the different SAP/X resins, compared to the weight as printed. The cubes were dried after printing for 24 h in a vacuum desiccator and subsequently swollen in a series of solutions with descending salt concentrations for 24 h each.

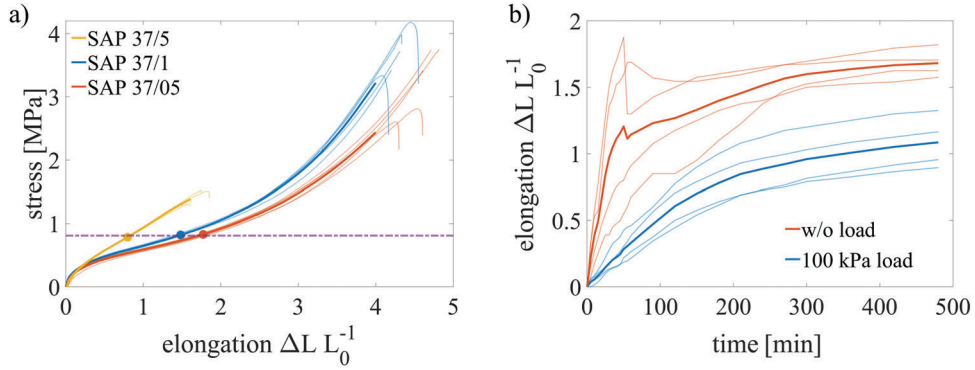

Figure 4. a) Stress–strain curves of printed SAP 37/X test rods during tensile testing at 2 min^{-1} elongation rate until breakage. The solid curves show the mean value of each group while the translucent lines represent individual samples (applies to (b), too). The dots show the intersection point of the curves with the calculated mean elongation during swelling measurements in water. The elongation was obtained from measurements in Figure 3. The size change was related to the mass change via a cubic relationship and the density of water. The purple line displays the mean stress value of the intersection points. b) Normalized thickness change of 2 mm thick 100 mm^2 SAP 37/1 disks over time during swelling in water. Red curves show the swelling of the material without an external load, while in the blue curves, the disks had a 10 N external load against the measured swelling.

respectively. As expected, the water uptake in the salt solutions (2 M NaCl and PBS) was lower than in pure water, showing the role of the osmotic pressure for the swelling (Figure 3). The swelling of the SAP 37/05 is still far from the 285-fold water absorption capacity of commercial sodium polyacrylate superabsorbent materials. This could be due to the commonly used solution polymerization for commercial applications resulting in linear, separated chains. The linear but more tangled chains obtained during printing might restrict extensive swelling behavior.[40,48,49]

A characteristic of superabsorbent materials is that they can strongly swell against an external load. This strong swelling is advantageous in 4D printing applications when something needs to be mechanically actuated. In equilibrium, the force (F_Π) generated by the osmotic pressure balances the elastic force generated by the network ($F_{elastic}$). With an additional external load ($F_{external}$), the forces therefore equilibrate as:[36,51]

$$F_\Pi = F_{elastic} + F_{external} \quad (1)$$

The elastic component can be determined from the stress–strain relationship obtained in a tensile test. However, this relationship is an approximation since it only represents a load in 1D, while swelling is a 3D process. For the tests, we printed tensile test rods from the three superabsorbent materials SAP 37/X, having a different crosslinker content (SAP 37/1, SAP 37/05, SAP 37/5). The measured stress–strain ($\Delta l\ l_0^{-1}$) curves are given in **Figure 4**a. Initially, all materials show a stiff stress–strain relation. Starting from elongations of ≈0.2, however, a flattening of the curves indicates a soft elastic region. With higher elongations (>3), the materials' stiffness increases until they brake (Table S2, Supporting Information). As expected, the different materials get stiffer and less extensible with a higher crosslinking degree since the crosslinks limit the length increase of the entangled chains. Overall, the elongation at break was found as $\Delta l\ l_0^{-1} = 1.6 \pm 0.1$, 4.6 ± 0.2 and 4.3 ± 0.1 for the SAP 37/5, SAP 37/1 and the SAP37/05, respectively. Similarly, an engineering stress of 1.4 ± 0.1, 3.2 ± 0.5, and 3.7 ± 0.3 MPa (SAP 37/5, SAP 37/1, and

SAP37/05, respectively) showed a decrease in stretchability with an increase in crosslinking. The initial region where the material changes its characteristic from stiff to soft is in good accordance with the pre-swelling in saturated NaCl, helping to render the dried prints flexible again.

Since the concentration of soluble Na^+ ions is the same in all SAP 37/X formulations, the osmotic pressure can be assumed to be similar.[36] From Equation (1), we know that without external stress, the osmotic force is equal to the elastic relaxation force of the polymer network. Therefore, the elastic stress in the hydrogel should be similar for all SAP 37/X prints with different degrees of crosslinking at an equilibrium swelling state. We confirmed this assumption from the measured stress–strain curves shown in Figure 4. To find the relevant elongation for each material, we used the results from the swelling tests shown in Figure 3. We converted the measured change in mass to the elongation via a cubic relation and the density of water. The relevant elongation for each material is indicated (colored dots) in Figure 4a. As expected, the corresponding stress values of 820 ± 40, 830 ± 50, and 780 ± 30 kPa (SAP 37/5, SAP 37/1, and SAP37/05, respectively) were similar with a mean of 810 ± 60 kPa (maximum absolute errors). Under the assumptions made, the superabsorbent prints could perform a movement during swelling against an external load up to a pressure of ≈810 kPa. The resulting force by this pressure is usually referred to as an actuator's blocking force.[36,52]

To validate this force stroke relation, we recorded the swelling of 2 mm thick SAP 37/1 discs (radius of 5.6 mm) in water without and with an external load (100 kPa) over a time of 8 h. From the stress–strain curve in Figure 4a, a 100 kPa load is expected to decrease the relative elongation to 1.2 ± 0.2. Figure 4b shows the measured increase in thickness over time. The red curve shows a significant swelling of the disks without external load, equilibrating after 8 h. The strong variation in the change during the initial 30 min is caused by warpage because of non-uniform swelling. This buckling is prevented and flattened by the external 100 kPa load in the blue curves. As expected, the approximately constant thickness changes of $\Delta l\ l_0^{-1} = 1.7 \pm 0.1$ for the swelling without load are higher than 1.1 ± 0.2 with the external load (mean and standard deviation $n = 4$). Within its standard deviation, this value is consistent with the prediction above. It shows that the hydrogel can still perform 65% of the swelling stroke with a 100 kPa load. The other PNIPAm-based hydrogel actuators already show no swelling at lower external loads of 80 and 10 kPa.[9,36] This high actuator's stroke under load is a key advantage of our 3D printed sodium polyacrylate superabsorbent polymer compared to other 4D printing resins.

2.4. Biocompatibility

Biomedical applications can benefit from the printable superabsorbent hydrogel to fabricate miniaturized, soft, self-deforming parts such as the shown stent structure. A critical material property for biomedical applications is compatibility with biologic tissue. One essential indicator of biocompatibility is cytotoxicity, that is, whether the material negatively affects cell growth. Therefore, materials are usually tested in vitro to assess their biocompatibility. Sodium polyacrylate hydrogels are already reported to be cytocompatible in literature.[53] However, not fully polymerized acrylic acid monomers and unreacted photo initiators could still harm the cells. The open network and the high-water content in the swollen hydrogel can promote the diffusion of such harmful molecules into the cells' environment. To avoid this problem, we post-cured the material after printing to polymerize the unreacted groups. Furthermore, the printed cubes were immersed in cell culture medium for seven days to remove the remaining soluble cytotoxic components.

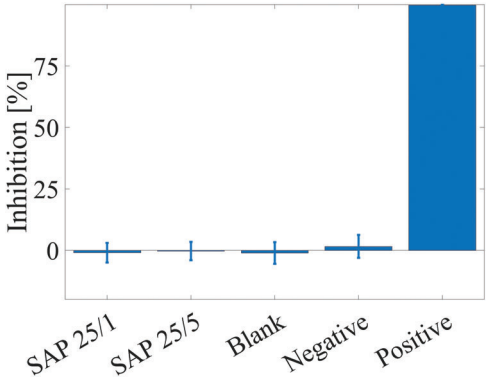

Figure 5. Inhibition of cell metabolism in a WST8 cytotoxicity test using eluates of neutralized and pre-extracted superabsorbent 5 mm cubes with polypropylene tubes as negative and SAP 37/1 with 5% zinc salt as the positive control.

Another problem is that partially neutralized acrylic acid shifts the pH-value of the cell culture medium to more acidic values, which is unfavorable for cell survival. To address this issue, we soaked the prints in 0.5% NaOH in PBS solution for 24 h before extraction, neutralizing the remaining polyacrylic acid and thus keeping the culture medium in a suitable range. After the pre-treatment of the prints, the metabolism of cells exposed to the SAP 37/X eluates was compared to blank and negative reference samples using the 2-(2-methoxy-4-nitrophenyl)-3-(4-nitrophenyl)-5-(2,4-disulfophenyl)-2H-tetrazolium monosodium (WST-8) eluate test (cell inhibition shown in **Figure 5**). The material did not show cytotoxic behavior in this test and could therefore potentially be used in biomedical applications.[54]

2.5. 4D Printing

To illustrate the applicability in multi-material 4D printing, we designed a self-folding tetrahedron shown in **Figure 6**. The SAP 37/5 (purple in Figure 6a) was printed between the thicker sidewalls as a bilayer onto a layer of commercial flexible resin to form a hinge. The superabsorbent resin swells in water, creating stress against the flexible non-swelling layer. This stress is released by the structure folding along the edge (see Figure 6b,c and Video S2, Supporting Information). Compared to other printed folding bilayers, the 3D printed superabsorbent resin swells strongly even under counter-pressure, allowing smaller folding radii. Future research could address how the thicknesses of the flexible non-swelling layer and the swelling superabsorbent polymer influence the folding.

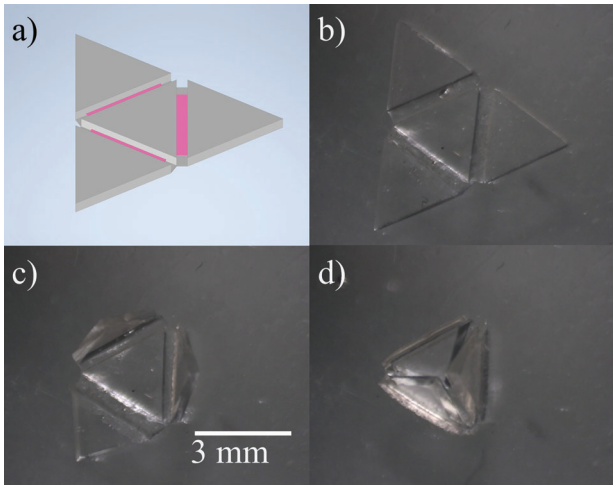

Figure 6. a) CAD design of a foldable tetrahedron printed from two materials. Structures which are printed with flexible resin are displayed in gray. Structures which are printed in between the flexible resin layers with SAP 37/5 are indicated in magenta. c–e) The microscope images show the folding process. When the print is immersed in water, the superabsorbent polymer swells and actuates the folding from a flat structure to a tetrahedron.

3. Conclusion and Outlook

In summary, we have shown a simple formulation for a reproducible SLA printable superabsorbent resin. The sodium acrylate units in the polymer generate an internal osmotic pressure when immersed in water. This allows the material to swell over 20 times its initial weight even against an external load (65% remaining stroke at 100 kPa load). Furthermore, it is printable with low water content, cytocompatible, and easily combined with other materials in printing. These properties make it an optimal candidate for 4D printing applications when large deformations or exertion of forces in contact with water are needed. Depending on future applications, variations of the mixture presented in this work are conceivable. The formulation may be changed to study the effect of different neutralization degrees or co-polymers with other materials like chitosan.[55–57] Further surface crosslinking of the printed part could ensure an equal swelling in parts with changing wall diameters.[48] Furthermore, complex printed structures like foldable parts could be fabricated in combination with other deformable materials such as silicones.[44,58,59]

4. Experimental Section

Materials: Acrylic acid (AA), 2-hydroxyethyl methacrylate (HEMA), sodium hydroxide (anhydrous; NaOH), poly(ethylene glycol) diacrylate (PEGDA, M_n 525), 2,2,6,6-tetramethylpiperidine-1-oxyl (TEMPO), phosphate-buffered saline (PBS), calcium alginate, sodium alginate, sodium chloride (NaCl), Dulbecco's modified Eagle's medium (DMEM), fetal bovine serum, l-glutamine, penicillin, streptomycin, and trypsin were purchased from Sigma Aldrich (USA). 2-Propanol (≥99.5%) and ethanol (≥99.5%) were obtained from Carl Roth (Germany). B(2,4,6-trimethylbenzoyl)phenylphosphine oxide/ethyl(2,4,6-trimethylbenzoyl)phenylphosphinate (Omnirad 2100) as photoinitiator blend and 2-isopropylthioxanthone (ITX) as UV-absorber was obtained from IGM Resins (Netherlands). The flexible 3D printing resin luxaprint flex was obtained from Detax (Germany). Deionized water was generated by an Ultra Clear purification system (Evoqua Water Technologies, Germany). For the biocompatibility testing, a CK04-13 CELL COUNTING KIT-8 from GERBU Biotechnik (Germany) was used. 96-well tissue culture plates were obtained from TTP Techno Plastic Products (Switzerland). 50 mL centrifuge tubes (Falcon, Corning Life Science), 2 mL centrifuge tubes (Safelock, Eppendorf), 76 × 52 × 1 mm^3 microscopy slides (Marienfeld), and cleanroom wipes (ReFIBE, Contec) were purchased from VWR (USA).

Resin Preparation: We prepared the resin as batches in 50 mL tubes as follows. First, the authors mixed the acrylic acid (23 g) with the HEMA (11.5 g). Then, the sodium acrylate was generated by neutralizing the acrylic acid with sodium hydroxide. To this end, they mixed dropwise the sodium hydroxide solution (15.5 g) of to the acrylic acid, HEMA mixture (34.5 g) under vigorous stirring. This resulted in a stable reaction without crystallization of the sodium acrylate or an introduced polymerization of the acrylic acid through the heat of the reaction, as observed for higher concentrations of sodium hydroxide. After the solution cooled down to room temperature, they added PEGDA 525 (0.5%, 1%, and 5%) to the base monomer mixture as a crosslinker and Omnirad 2100 (1%), ITX (0.05%), and TEMPO (0.02%) as the printing additives (w/w). Finally, the resin was homogenized by sonication (30 min, Branson 5510, USA) until the ITX powder was dissolved and stored dark until usage. The resin compositions are summarized in Table S1, Supporting Information.

Printing Conditions: The authors printed the resin using a Miicraft 50X (Miicraft, Taiwan) SLA printer. The printer features an inverted setup with a 365 nm wavelength UV exposure through a dynamic mirror array from the bottom. The authors chose 10 s exposure time with an increased base exposure of 30 s for the first layer and 3 mW cm^{-2} (300%) as printing parameters. To remove the prints, they attached a glass slide (76 × 52 mm^2) with a calcium alginate sacrificial layer onto the picker using adhesive tape (Tesa, Germany). To improve the adhesion of sodium alginate, the glass was hydrophilized in O_2 plasma (Diener Femto 90%, 0.8 mbar oxygen, Diener, Germany) for 5 min. after which a solution of sodium alginate (1 M) was spin-coated (Polos SPIN 200, 2000 min^{-1} for 45 s, SPS-Europe B.V., Netherlands) and dried with pressurized air. Next, the sodium alginate layer was gelled by immersion into a calcium alginate solution (0.5 M), rinsed with water, and dried again with pressurized air.

After detaching the prints from the glass slide, they were alternately rinsed with deionized water and ethanol, ending with ethanol to prevent swelling. To fully polymerize the samples, the prints were post-cured in a UV chamber (Otoflash G171, NK-Optik, Germany) using 2000 flashes under nitrogen flux. They were stored dry and, if not stated otherwise, were preconditioned to regain their flexibility in a saturated NaCl solution (5.4 M) for 24 h prior to experiments.

The parts were designed with the computer-aided design (CAD) drawing software Inventor 2022 and Meshmixer (Autodesk, USA), exported as stl-format, and sliced at 50 µm height with the printer control software MiiUtility (Miicraft Taiwan).

Swelling Characterization: The swelling capability of the different resin compositions was analyzed by measuring the mass difference of printed 5 mm cubes. The cubes were first dried in a vacuum for 24 h (MD 1, 1.5 mbar, Vacuubrand, Germany), and subsequently immersed in solutions with decreasing salt concentrations. After a drying or swelling period of 24 h, excess water was removed from the cubes with a paper towel and the cubes' weight was determined (Sartorius CP225D, Germany). The change of mass (Δm) was compared to the initial mass after printing (m_0) as relative change in mass ($\Delta m\, {m_0}^{-1}$). The mean value of 15 separate cubes, and the standard deviation was calculated using Gaussian error propagation. For comparison, the mass change was converted to a change in length using a cubic relation and the density of the absorbed water.

3D-Structure Fabrication: We printed a 3D -design of a ship known as "Benchy" in the printing community. The original model was reduced in size to a length of 15 mm and made hollow for a maximum wall thickness of 1 mm. It was transferred into the bottle in the dry state and swollen in water with 1% ink (Lamy, Germany) for 24 h to stain it blue. Subsequently, the colored water was replaced by clear water to make the ship visible inside the bottle. A second 3D structure resembling a medical stent was

composed of a mesh-like hollow cylinder with a diameter of 7.2 mm, a height of 9.6 mm, and a wall thickness of 1.2 mm (details shown in Figure S4, Supporting Information).

Mechanical Characterization: The material's flexibility is essential for deformable structures in a 4D printing approach. Thus, the authors conducted tensile tests following a standard protocol ISO 527-1:2012. They printed the test specimens with a cross-section of 3.33×2 mm^2 and a length of 50 mm oriented parallel to the build platform. The structure had a tapered gauge length of 20 mm, as shown in Figure S6, Supporting Information. They performed the tests on a Zwick Z2.5 (Zwick-Roell, Germany) universal testing machine with 40 mm min^{-1} (twice initial gauge length per minute) tensile speed until breakage.

To examine the ability to swell against an external force, the authors recorded the thickness increase of a printed disc in water with and without external load over 8 h using a dial indicator (Wabeco, Germany). They printed the discs from SAP 37/1 with 2 mm thickness and a radius of 5.6 mm. For the measurement with an external load, they applied 10 N with a weight on the disk, equivalent to a pressure of 100 kPa on the surface. To ensure wetting of the superabsorbent polymer from both sides, top and bottom, a piece of tissue (Cleanroom Wipes) also soaked in water, which can be considered incompressible in this context, was put under and on top of the superabsorbent disk. A picture and schematic of the setup are displayed in Figure S7, Supporting Information.

Biocompatibility: Biocompatibility of the material is an essential characteristic for potential biomedical applications in contact with living tissue. As one of the critical factors, the authors tested the cytotoxicity of the material. The experiments were conducted following the ISO 10993-5:2009 and ISO 10993-12:2012 standard as an eluate test using a WST-8 assay, which measures the cell viability via inhibition of the dehydrogenase activity. They used HT1080 cells as a test cell line. The cells were cultured in Dulbecco's modified Eagle's medium (DMEM) supplemented with fetal bovine serum (10% v/v), penicillin/streptomycin (100 U ml^{-1}/0.1 mg ml^{-1}), and L-glutamine (2 mM), in a humidified incubator at 37 °C and 5% CO_2. For passaging after confluence, the cells were detached with 0.5% Trypsin-EDTA. They used 3D printed 5 mm cubes of the SAP 37/1 and SAP 37/5 materials as samples. A 2 mL polypropylene tube served as a negative control and an SAP 37/5 cube with 5% zinc chloride as a positive control. The samples were immersed in PBS with 0.5% NaOH for 24 h and then extracted in cell culture media for one week to stabilize the pH and extract possible toxic not cured monomers. The preconditioned samples were first disinfected by dipping them into 2-propanol solution (70%) and drying for 1 h. Then, the samples were stored in 50 mL tubes (to fit the swollen samples) with the cell culture medium adjusted to 25 mL volume in the incubator for 96 h to produce the eluates. The medium for blank control was also stored under the same conditions. The HT1080 cells were seeded onto 96-well cell-culture plates with 4k cells per well. After initial culturing for 24 h, the medium was replaced with the eluates and incubated for 72 h. Then, the cell activity was measured via a colorimetric assay and compared to the activity of cells supplied with the control culture media. To this end, the WST-8 stock solution was added to the media in the wells in a 1:10 (v/v) ratio and the samples were incubated for 1 h. After the incubation, the absorption of the media was measured with an ELISA photometer (Sunrise, Tecan Group, Switzerland) at 450 and 620 nm. Blank measurements of wells without cells were also included to correct the readings for potential color changes of the eluates. The inhibition of cell metabolism is calculated by:

$$\text{Inhibition} = 1 - \frac{(A - A_b)}{(A_c - A_{cb})} \tag{2}$$

where A_c is the absorption of the control culture supplied with fresh media, A_{cb} is the absorption of the fresh media without cells, A is the absorption of the tested cell culture supplied with eluates and A_b is the blank eluate absorption. The mean was calculated for 8 cell culture wells per eluate and three eluates produced with each superabsorbent polymer mixture. The error is the standard deviation propagated as Gaussian error.

Folding Structure: The folding structure was composed of 4 equilateral triangles with a 4.5 mm side length connected with a joint bridge of 0.45 mm at the edges, as shown in Figure S8, Supporting Information. The part was printed by combining the swelling superabsorbent resin and a commercial flexible resin (luxaprint flex). First, one layer (50 µm thickness) of the flexible resin was printed, forming the triangles and the connection in the joints. Then, the build platform was cleaned with 2-propanol, and the resin tank was changed to the SAP 37/5 resin. Next, the actuating superabsorbent layer (50 µm) was printed in the joint area, followed by cleaning with water and ethanol and switching the resin back to the flexible resin. Then the rest of the triangles were printed to reach a total thickness of 350 µm. Finally, the folding was performed in deionized water under a stereomicroscope (BMS Microscopes, Netherlands) and recorded with an optical camera (Canon M5, Japan).

Supporting Information

Supporting Information is available from the Wiley Online Library or from the author.

Acknowledgements

The authors would like to acknowledge Kilian Müller and Petra Mela at Technische Universität München for their support with tensile testing. The work was funded by the Bavarian Ministry for Science and the Art through the ONE MUNICH Project "Munich Multiscale Biofabrication".

Open access funding enabled and organized by Projekt DEAL.

Conflict of Interest

The authors declare no conflict of interest.

Data Availability Statement

The data that support the findings of this study are available from the corresponding author upon reasonable request.

Keywords

4D printing, shape transformation, sodium acrylate, superabsorbent polymers, stents, stereolithography

Received: May 3, 2022
Revised: June 28, 2022
Published online: July 27, 2022

[1] M. Champeau, D. A. Heinze, T. N. Viana, E. R. de Souza, A. C. Chinellato, S. Titotto, *Adv. Funct. Mater.* **2020**, *30*, 1910606.
[2] H. Chu, W. Yang, L. Sun, S. Cai, R. Yang, W. Liang, H. Yu, L. Liu, *Micromachines* **2020**, *11*, 796.
[3] S. Magdassi, A. Kamyshny, *Nanomaterials for 2D and 3D Printing*, Wiley-VCH Verlag GmbH & Co. KGaA, Weinheim, Germany **2017**.
[4] K. Jung, N. Corrigan, M. Ciftci, J. Xu, S. E. Seo, C. J. Hawker, C. Boyer, *Adv. Mater.* **2020**, *18*, 1903850.
[5] S. Tibbits, *Archit. Des.* **2014**, *84*, 116.
[6] X. Kuang, D. J. Roach, J. Wu, C. M. Hamel, Z. Ding, T. Wang, M. L. Dunn, H. J. Qi, *Adv. Funct. Mater.* **2019**, *10*, 1805290.
[7] Y. Dong, S. Wang, Y. Ke, L. Ding, X. Zeng, S. Magdassi, Y. Long, *Adv. Mater. Technol.* **2020**, *5*, 2000034.
[8] A. B. Baker, S. R. G. Bates, T. M. Llewellyn-Jones, L. P. B. Valori, M. P. M. Dicker, R. S. Trask, *Mater. Des.* **2019**, *163*, 107544.

[9] M. Hua, D. Wu, S. Wu, Y. Ma, Y. Alsaid, X. He, *ACS Appl. Mater. Interfaces* **2021**, *13*, 12689.
[10] M. N. Shiblee, K. Ahmed, M. Kawakami, H. Furukawa, *Adv. Mater. Technol.* **2019**, *4*, 1900071.
[11] S. E. Bakarich, R. Gorkin III, M. in het Panhuis, G. M. Spinks, *Macromol. Rapid Commun.* **2015**, *36*, 1211.
[12] Z. Ji, C. Yan, B. Yu, X. Zhang, M. Cai, X. Jia, X. Wang, F. Zhou, *Adv. Mater. Technol.* **2019**, *4*, 1800713.
[13] J. Liu, O. Erol, A. Pantula, W. Liu, Z. Jiang, K. Kobayashi, D. Chatterjee, N. Hibino, L. H. Romer, S. H. Kang, T. D. Nguyen, D. H. Gracias, *ACS Appl. Mater. Interfaces* **2019**, *11*, 8492.
[14] Z. Zhang, N. Corrigan, A. Bagheri, J. Jin, C. Boyer, *Angew. Chem., Int. Ed.* **2019**, *58*, 17954.
[15] D. Kim, T. Kim, Y.-G. Lee, *J. Vis. Exp.* **2019**, *149*, e59746.
[16] P. Morouço, B. Azimi, M. Milazzo, F. Mokhtari, C. Fernandes, D. Reis, S. Danti, *Appl. Sci.* **2020**, *10*, 9143.
[17] A. S. Gladman, E. A. Matsumoto, R. G. Nuzzo, L. Mahadevan, J. A. Lewis, *Nat. Mater.* **2016**, *15*, 413.
[18] J. M. Taylor, H. Luan, J. A. Lewis, J. A. Rogers, R. G. Nuzzo, P. V. Braun, *Adv. Mater.* **2022**, *34*, 2108391.
[19] C. Yang, J. Luo, M. Polunas, N. Bosnjak, S.-T. D. Chueng, M. Chadwick, H. E. Sabaawy, S. A. Chester, K.-B. Lee, H. Lee, *Adv. Mater.* **2020**, *32*, 2004285.
[20] A. Kotikian, J. M. Morales, A. Lu, J. Mueller, Z. S. Davidson, J. W. Boley, J. A. Lewis, *Adv. Mater.* **2021**, *33*, 2101814.
[21] Z. Zhao, X. Kuang, C. Yuan, H. J. Qi, D. Fang, *ACS Appl. Mater. Interfaces* **2018**, *10*, 19932.
[22] L. Huang, R. Jiang, J. Wu, J. Song, H. Bai, B. Li, Q. Zhao, T. Xie, *Adv. Mater.* **2017**, *29*, 1605390.
[23] D. Han, Y. Wang, C. Yang, H. Lee, *ACS Appl. Mater. Interfaces* **2021**, *13*, 12735.
[24] D. Han, Z. Lu, S. A. Chester, H. Lee, *Sci. Rep.* **2018**, *8*, 1963.
[25] T. Uchida, H. Onoe, *Micromachines* **2019**, *10*, 433.
[26] Y. Wang, N. Alizadeh, M. Barde, M. L. Auad, B. S. Beckingham, *ACS Appl. Polym. Mater.* **2022**, *4*, 971.
[27] D. Morales, E. Palleau, M. D. Dickey, O. D. Velev, *Soft Matter* **2014**, *10*, 1337.
[28] K. E. Engel, P. A. Kilmartin, O. Diegel, *Polym. Chem.* **2022**, *13*, 456.
[29] D. Han, C. Farino, C. Yang, T. Scott, D. Browe, W. Choi, J. W. Freeman, H. Lee, *ACS Appl. Mater. Interfaces* **2018**, *10*, 17512.
[30] C. Garcia, A. Gallardo, D. López, C. Elvira, A. Azzahti, E. Lopez-Martinez, A. L. Cortajarena, C. M. González-Henríquez, M. A. Sarabia-Vallejos, J. Rodríguez-Hernández, *ACS Appl. Bio Mater.* **2018**, *1*, 1337.
[31] A. Kirillova, R. Maxson, G. Stoychev, C. T. Gomillion, L. Ionov, *Adv. Mater.* **2017**, *29*, 1703443.
[32] L. Larush, I. Kaner, A. Fluksman, A. Tamsut, A. A. Pawar, P. Lesnovski, O. Benny, S. Magdassi, *J. 3D Print. Med.* **2017**, *4*, 219.
[33] T. L. Sun, T. Kurokawa, S. Kuroda, A. B. Ihsan, T. Akasaki, K. Sato, M. A. Haque, T. Nakajima, J. P. Gong, *Nat. Mater.* **2013**, *12*, 932.
[34] J.-Y. Sun, X. Zhao, W. R. K. Illeperuma, O. Chaudhuri, K. H. Oh, D. J. Mooney, J. J. Vlassak, Z. Suo, *Nature* **2012**, *489*, 133.
[35] S. Dutta, D. Cohn, *J. Mater. Chem. B* **2017**, *5*, 9514.
[36] W. R. K. Illeperuma, J.-Y. Sun, Z. Suo, J. J. Vlassak, *Soft Matter* **2013**, *9*, 8504.
[37] K. Horie, M. Baron, R. B. Fox, J. He, M. Hess, J. Kahovec, T. Kitayama, P. Kubisa, E. Maréchal, W. Mormann, R. F. T. Stepto, D. Tabak, J. Vohlídal, E. S. Wilks, W. J. Work, *Pure Appl. Chem.* **2004**, *76*, 889.
[38] F. Horkay, I. Tasaki, P. J. Basser, *Biomacromolecules* **2000**, *1*, 84.
[39] K. J. Buchanan, B. Hird, T. M. Letcher, *Polym. Bull.* **1986**, *15*, 325.
[40] R. Mahon, Y. Balogun, G. Oluyemi, J. Njuguna, *SN Appl. Sci.* **2020**, *2*, 117.
[41] J. Misiewicz, K. Lejcuś, J. Dąbrowska, D. Marczak, *Sci. Rep.* **2019**, *9*, 18098.
[42] A. Bagheri, C. M. Fellows, C. Boyer, *Adv. Sci.* **2021**, *8*, 2003701.
[43] A. A. Pawar, G. Saada, I. Cooperstein, L. Larush, J. A. Jackman, S. R. Tabaei, N.-J. Cho, S. Magdassi, *Sci. Adv.* **2016**, *2*, e1501381.
[44] S. Zips, L. Hiendlmeier, L. J. K. Weiß, H. Url, T. F. Teshima, R. Schmid, M. Eblenkamp, P. Mela, B. Wolfrum, *ACS Appl. Polym. Mater.* **2021**, *3*, 243.
[45] O. Wichterle, D. Lim, *Nature* **1960**, *185*, 117.
[46] R. Zhang, N. B. Larsen, *Lab Chip* **2017**, *17*, 4273.
[47] T. F. Teshima, L. Hiendlmeier, K. Terkan, S. Zips, L. Grob, F. Zurita, P. Rinklin, B. Wolfrum, *Adv. Mater. Technol.* **2021**, *9*, 2100240.
[48] L. Arens, D. Barther, J. Landsgesell, C. Holm, M. Wilhelm, *Soft Matter* **2019**, *15*, 9949.
[49] N. Bel'nikevich, T. V. Budtova, S. A. Vesnebolotskaya, G. K. Elyashevich, *Russ. J. Appl. Chem.* **2008**, *81*, 1818.
[50] S. Morita, *Front. Chem.* **2014**, *2*, 10.
[51] F. Oveissi, D. F. Fletcher, F. Dehghani, S. Naficy, *Mater. Des.* **2021**, *203*, 109609.
[52] H. Kim, J. Ma, M. Kim, J. Nam, K.-U. Kyung, *Adv. Intell. Syst.* **2021**, *3*, 2100006.
[53] J.-W. Li, Y.-J. Li, X.-S. Hu, Y. Gong, B.-B. Xu, H.-W. Xu, Z.-Q. Yin, *Int. J. Ophthalmol.* **2020**, *13*, 1521.
[54] International Organization for Standardization, **2009**, *ISO 10993–5:2009*.
[55] M. He, L. Shi, G. Wang, Z. Cheng, L. Han, X. Zhang, C. Wang, J. Wang, P. Zhou, G. Wang, *Int. J. Biol. Macromol.* **2020**, *155*, 1245.
[56] D. R. Barleany, R. S. D. Lestari, M. Yulvianti, T. R. Susanto, Shalina, Erizal, *Int. J. Adv. Sci. Eng. Inf. Technol.* **2017**, *2*, 702.
[57] J. D. Schneible, A. T. Young, M. A. Daniele, S. Menegatti, *Pharm. Res.* **2020**, *37*, 142.
[58] N. Bhattacharjee, C. Parra-Cabrera, Y. T. Kim, A. P. Kuo, A. Folch, *Adv. Mater.* **2018**, *30*, 1800001.
[59] Q. Ge, A. H. Sakhaei, H. Lee, C. K. Dunn, N. X. Fang, M. L. Dunn, *Sci. Rep.* **2016**, *6*, 31110.

